The Triangle Sky: Canonical Apices, Triangle Strands, and Orthocentric Completions

Ismail Hammoudeh

Pilot manuscript v0.3.0 — 6 September 2026

Abstract

A fixed triangle provides a natural reference face for studying tetrahedral geometry. We organize similarity-equivariant apex constructions as mirror pairs, called triangle stars, and one-parameter families of such pairs as triangle strands. Three fixed-base optimization problems admit complete solutions: the circumsphere-volume and insphere-volume objectives have unique optimizers for every nondegenerate base, whereas the edge-variance optimizer exists precisely when the mean base edge exceeds the circumradius. We also prove existence, without asserting uniqueness, for the circumradius-to-inradius objective. Power-additive tetrahedra have an explicit strand parametrization by an edge potential; every exponent greater than one gives an unbounded admissible tail over every base triangle. Exact trace formulas explain the persistence of affine center families and Euler-line coincidences. An identity separates the dihedral-angle defect into normal-frame anisotropy and a first-moment defect. Finally, orthocentric completions in four-dimensional Euclidean space yield canonical twin apices, explicit projected incenters, and a center-proximity selection with a controlled right-triangle degeneration. The resulting theorems provide a mathematical foundation for a larger experimental catalogue, whose numerical center identifications and heuristic rankings are kept distinct from proof.

Keywords: triangle center; tetrahedron; geometric optimization; apex locus; orthocentric simplex; tight frame.
MSC 2020: 51M04, 51M20, 52B10.

1 Introduction

Fix a nondegenerate triangle ABC in a Euclidean plane. A tetrahedron with this face is determined by the foot P of its fourth vertex and its nonzero height h. This elementary decomposition permits two complementary questions: which geometric conditions select a canonical apex, and which conditions leave a curve of possible apices? The former produce triangle centers together with invariant heights; the latter produce the *triangle strands* considered here.

The starting point is the living Triangle Sky report [1]. That report combines a catalogue of spatial constructions, numerical triangle-center searches, optimization candidates, and an extension to 4-simplices. The present paper extracts its structural results and supplies global arguments and domain conditions where the report gave stationary or numerical evidence. It also develops a strand formulation motivated by fixed-face visualization. The report remains the detailed experimental supplement; the mathematical conclusions here do not depend on the completeness of its database search.

Triangle-center functions and their naming conventions follow Kimberling [3, 4]. Fixed-apex optimization has a substantial predecessor in mesh smoothing [6]. In particular, the fixed-height surface-area minimization used below already appears in Colognese and Pollicott [7]; we include a short proof to handle arbitrary exterior feet and to optimize the height as well. Orthocentric-simplex theory supplies the higher-dimensional background [8]. Our normal-frame comparison uses the standard frame-potential setting [9, 10], but its admissible normals are constrained to come from a tetrahedron with a prescribed face. Unconstrained frame-optimization theorems therefore do not resolve that fixed-face problem.

The main contributions are the domain-complete optimization statements in Section 3, the explicit strand and admissibility theorem in Section 5, and the common treatment of trace closure and orthocentric completion in Sections 6 and 7. These results are assembled with self-contained proofs. We do not assert that every individual classical construction or elementary identity is new, or that the underlying catalogue is complete.

2 Stars, equivariance, and elementary controls

Write $a = |B - C|$, $b = |C - A|$, $c = |A - B|$, $s = (a + b + c)/2$, and let Δ, r, R be the area, inradius, and circumradius of ABC. Its centroid, incenter, circumcenter, and orthocenter are G, I, O, H. Fix a unit normal n temporarily.

Definition 2.1. On a similarity- and permutation-invariant domain of triangles, a *triangle star* is a rule

$$\mathcal{S}(ABC) = \{P + hn, P - hn\}, \qquad h > 0,$$

where P is a similarity-equivariant, label-independent point and h^2 is a symmetric function homogeneous of degree two in the side lengths. The point P is its *foot*. A zero height is a boundary value, not a nondegenerate tetrahedral star.

A center is allowed to be exterior to the triangle. Negative barycentric coordinates are not replaced by absolute values. Complex algebraic continuations may be useful computationally, but they are not real Euclidean stars.

Proposition 2.2 (Selection and projection)**.** *An intrinsic, similarity-covariant construction invariant under base relabelling defines a star whenever it selects a unique apex modulo reflection in the base plane. More generally, a uniquely selected completion modulo isometries fixing the base produces a triangle center by projecting any canonical, similarity-equivariant center of that completion.*

Proof. A similarity or relabelling sends a selected completion to an admissible completion with the same defining property. Uniqueness identifies it with the selected completion for the transformed base, modulo the allowed isometries. Those isometries fix horizontal projections. The projected point is therefore equivariant; squared normal lengths scale quadratically. ☐

An equivariant *set* of several minimizers does not by itself select an individual triangle center. Likewise, a symmetric apex curve need not be a globally labelled one-parameter collection of stars: a compatible parameter and branch rule must be supplied.

It is useful to reserve a signed invariant distinct from a positive height:

$$\chi = (H - A) \cdot (H - B) = 4R^2 - \frac{a^2 + b^2 + c^2}{2} = -\frac{\sigma_A \sigma_B \sigma_C}{4\Delta^2}, \quad \sigma_A = \frac{b^2 + c^2 - a^2}{2}, \tag{1}$$

with cyclic definitions. The three products at H are equal by the altitude equations. The middle identity follows on putting $O = 0$ and $H = A + B + C$; the last follows by substituting the circumradius and Heron formulas. Thus $\chi < 0$, $= 0$, or > 0 according as the triangle is acute, right, or obtuse.

Proposition 2.3 (Orthogonal and equifacial stars)**.** *The apex with three mutually perpendicular incident edges has foot H and height $\sqrt{-\chi}$. The apex forming a disphenoid with ABC has foot $L = 2O - H$ and height $2\sqrt{-\chi}$. Both exist as nondegenerate real tetrahedra exactly for acute bases. Their tetrahedral centroids have feet $(3G + H)/4 = (O + H)/2$ and $(3G + L)/4 = O$, respectively, and one quarter of the corresponding apex heights.*

Proof. The differences of the equations $(D-A)\cdot(D-B)=0$, cyclically, force the foot of D to be H. The common product is then $\chi+h^2$. For the disphenoid put $O=0$, so $L=-H$. Its prescribed opposite-edge lengths require $|D-A|=a$, cyclically. These hold at $D=(-H,2\sqrt{-\chi})$, since $|H+A|^2-4\chi=a^2$ and its cyclic analogues. Squared-distance differences uniquely determine the foot and then the squared height, so no other real branch is missed. The centroid formulas use $3G=2O+H$. □

The classical names of these feet include $L=X(20)$ and $(O+H)/2=X(5)$. The displayed geometry, rather than a database match, establishes their identities.

3 Global fixed-base optimization

Throughout this section the domain is the full open half-space

$$D=P+hn, \qquad P\in \operatorname{aff}(ABC), \quad h>0.$$

Write $V_T=\Delta h/3$, R_T, r_T, and S_T for tetrahedral volume, circumradius, inradius, and total surface area. The statistical variance below uses divisor six; changing it does not change a minimizer.

Theorem 3.1 (Three explicit optima)**.** *The following statements hold over every nondegenerate base triangle.*

1. *The objective R_T^3/V_T has a unique minimizer, with $P=O$ and $h=\sqrt{2}R$.*
2. *The objective r_T^3/V_T has a unique maximizer, with $P=I$ and $h=2\sqrt{2}r$.*
3. *Put $m=(a+b+c)/3$. The variance of the six edge lengths has a nondegenerate minimizer if and only if $m>R$. In that case it is unique, with $P=O$ and $h=\sqrt{m^2-R^2}$. If $m\le R$, the infimum is attained only in the closed-half-space extension at height zero, and no nondegenerate optimizer exists.*

The corresponding sphere-volume ratios differ from the first two objectives only by the constant $4\pi/3$.

Proof. For the first assertion put $O=0$ in the base plane and write $p=P-O$. The tetrahedral circumcenter has horizontal component zero and vertical coordinate

$$z_O=\frac{|p|^2+h^2-R^2}{2h}, \qquad R_T^2=R^2+z_O^2.$$

For $0<h\le R$ the smallest possible R_T is R, attained when $|p|^2=R^2-h^2$; hence $R_T^3/h\ge R^2$. For $h\ge R$ the minimum over p is uniquely at $p=0$, giving

$$\frac{R_T^3}{h}=\frac{(h^2+R^2)^3}{8h^4}.$$

Its derivative changes sign only at $h^2=2R^2$. There the value is $27R^2/32<R^2$. This proves global optimality and uniqueness, including the previously considered smaller heights.

For the second assertion, let d_A,d_B,d_C be the signed distances from P to BC,CA,AB, positive inward. The signed area identity gives

$$ad_A+bd_B+cd_C=2\Delta=2sr.$$

The lateral face areas are $a\sqrt{h^2+d_A^2}/2$, cyclically. Strict convexity of $x\mapsto\sqrt{h^2+x^2}$ and the weights $a/(2s),b/(2s),c/(2s)$ yield

$$S_T\ge\Delta+s\sqrt{h^2+r^2}, \tag{2}$$

with equality precisely when all three signed distances equal r, that is, $P = I$. This is the fixed-height incenter principle; compare [7]. Since $r_T = 3V_T/S_T = \Delta h/S_T$, maximizing r_T^3/V_T at fixed h is equivalent to minimizing S_T. At $P = I$, putting $t = \sqrt{h^2 + r^2} > r$ reduces the objective, up to a positive constant, to

$$\frac{h^2}{(r + \sqrt{h^2 + r^2})^3} = \frac{t - r}{(t + r)^2}.$$

The derivative is $(3r - t)/(t + r)^3$. Its unique maximum is at $t = 3r$, or $h = 2\sqrt{2}r$.

For the last assertion, temporarily regard the three variable edge lengths $x_i = |D - A_i|$ as free variables. Apart from a constant, the variance is

$$\frac{x_1^2 + x_2^2 + x_3^2}{6} - \frac{(a + b + c + x_1 + x_2 + x_3)^2}{36}.$$

Its Hessian is $I_3/3 - \mathbf{1}\mathbf{1}^\mathsf{T}/18$, positive definite. Its unique stationary point is $x_1 = x_2 = x_3 = m$. Equal vertex distances force $P = O$ and $h^2 = m^2 - R^2$, proving the feasible case.

For $h > 0$, the Jacobian of $D \mapsto (x_1, x_2, x_3)$ is invertible: multiplying its rows by x_i gives the three independent vectors $D - A_i$, whose determinant has absolute value $2\Delta h$. Every interior stationary point must therefore be the free-variable one. If $m \le R$ there is none. Finally the variance tends to infinity as $|D| \to \infty$, because its variable part is a positive-definite quadratic form in (x_i). It extends continuously to $h \ge 0$ and attains a minimum there by compactness of sublevel sets. That minimizer must have $h = 0$ and is approachable from $h > 0$. This proves the boundary assertion without claiming boundary uniqueness. □

For example, $(a, b, c) = (1, 1, 19/10)$ gives $m = 13/10$ but $R = 10/\sqrt{39} > m$. Thus a real edge-variance star cannot be defined on all nondegenerate triangles. It is not enough to call its displayed radical an exact stationary solution.

Proposition 3.2 (Existence for the Euler ratio)**.** *For every fixed nondegenerate base, R_T/r_T attains a minimum at a nondegenerate tetrahedron. This statement does not assert uniqueness.*

Proof. Equation (2) implies $r_T \le r$, while $S_T \ge \Delta$ gives $r_T \le h$. Moreover $R_T \ge R$ by its horizontal circumcenter component, and R_T is at least half of each tetrahedral edge. On a sublevel set $R_T/r_T \le M$, these facts imply $h \ge R/M$ and every edge is at most $2Mr$. The apex is therefore bounded and bounded away from the base plane. Continuity gives compact sublevel sets within the nondegenerate domain and hence an attained minimum. □

Without uniqueness or an explicit equivariant selection, this supplies an invariant minimizer set, not a single Euler-ratio star.

4 Dihedral defects and normal isotropy

Let $n_0, \dots, n_3$ be the outward unit face normals and let δ_{ij} be the internal dihedral angle between the corresponding faces. Thus $n_i \cdot n_j = -\cos\delta_{ij}$. Define

$$\mathcal{D} = \sum_{i<j} (\cos\delta_{ij} - 1/3)^2, \quad \mathcal{F} = \left\| \sum_i n_i n_i^\mathsf{T} - \frac{4}{3} I_3 \right\|_F^2.$$

Theorem 4.1 (Exact defect decomposition)**.** *For every nondegenerate tetrahedron,*

$$\boxed{\mathcal{D} = \frac{1}{2}\mathcal{F} + \frac{1}{3}\left\| \sum_i n_i \right\|^2.} \tag{3}$$

Each defect vanishes exactly for regular tetrahedra. On equifacial tetrahedra the final term is zero, so $\mathcal{D} = \mathcal{F}/2$.

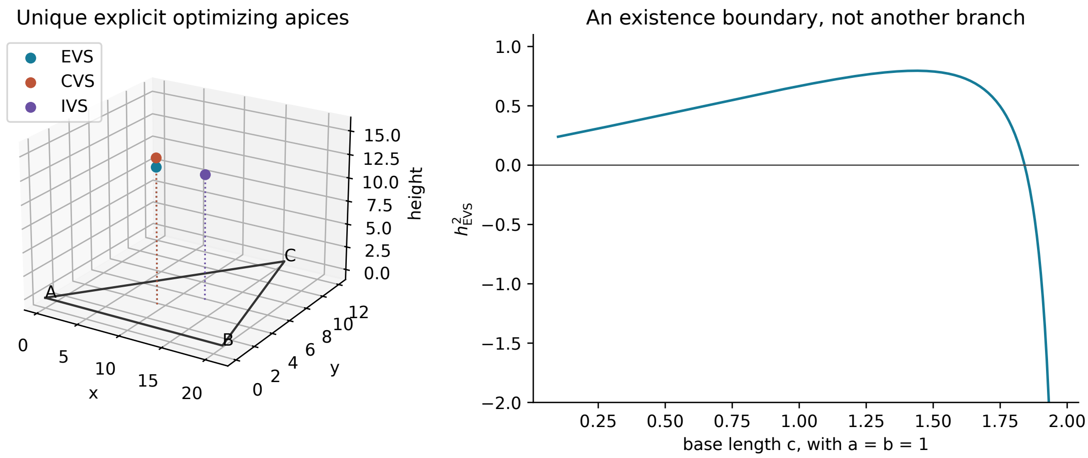

Figure 1: The three explicit optimizing apices above the acute 13–20–21 base (left). The isosceles bases $(1, 1, c)$ illustrate the edge-variance domain boundary (right): a negative squared height indicates nonexistence of a nondegenerate optimum, not a missing numerical branch.

Proof. Put $t_{ij} = n_i \cdot n_j$. Direct trace expansion gives

$$\mathcal{F} = 2\sum_{i<j} t_{ij}^2 - \frac{4}{3}, \qquad \left\|\sum_i n_i\right\|^2 = 4 + 2\sum_{i<j} t_{ij}.$$

Expanding $\mathcal{D} = \sum(t_{ij} + 1/3)^2$ proves (3). If $\mathcal{F} = 0$, the 3×4 normal matrix N has $NN^\mathsf{T} = 4I_3/3$. Its Gram matrix is $(4/3)(I_4 - vv^\mathsf{T})$ for a unit null vector v. Diagonal entries equal to one force $v_i^2 = 1/4$. The vector-area identity supplies a strictly positive null vector (the four face areas), so all $v_i = 1/2$ after choosing sign. Hence $t_{ij} = -1/3$ and all face areas are equal. The normals are those of a regular tetrahedron. Their four support numbers, modulo three translations, have one degree of freedom; thus the bounded tetrahedron is a translate and positive homothetic copy of a regular tetrahedron. Conversely a regular tetrahedron has both defects zero. The implication from $\mathcal{D} = 0$ also follows from (3). Finally equal face areas in $\sum F_i n_i = 0$ give $\sum n_i = 0$. $\square$

The frame potential is classical [9, 10]; the identity above explains precisely why the report's two objectives are related but are not interchangeable. It supplies neither coercivity nor uniqueness for their constrained minima. In particular, the fixed-base admissible normal set is not the whole space of unit frames.

5 Triangle strands and power-additive families

The dimension of a family of tetrahedra and the dimension of its ambient Euclidean space must be distinguished. Up to Euclidean isometry, labelled nondegenerate tetrahedra form an open subset of six-dimensional edge-length space. A four-dimensional *family* in that space still consists of tetrahedra in $\mathbb{R}^3$.

Definition 5.1. For a family $\mathcal{M}$ of tetrahedra, its *fixed-base apex locus* is

$$\mathcal{L}_{ABC}(\mathcal{M}) = \{D \notin \operatorname{aff}(ABC) : ABCD \in \mathcal{M}\}.$$

A one-dimensional smooth component modulo base reflection is an unparametrized *triangle strand*. An invariant parameter and equivariant branch selection make it a family of triangle stars on the parameter's admissible domain.

Proposition 5.2 (The dimension qualification)**.** *Let $\mathcal{M}$ be a smooth four-dimensional submanifold of labelled tetrahedral edge-length space. If the map recording the three base edges has rank three at a point, its local fixed-base fiber is a smooth curve. This conclusion need not hold at critical fibers.*

Proof. Apply the submersion theorem. For a fixed nondegenerate base, the map from an apex in the upper half-space to its three distances from A, B, C is a local diffeomorphism by the Jacobian calculation in Theorem 3.1. Thus the fiber dimension agrees with that of the apex locus. □

A dimension count alone says nothing about global connectedness, missing fibers, compactness, or permutation-compatible labelling of components.

5.1 A complete parametrization for power-additive tetrahedra

Fix $k > 0$. Say that a tetrahedron is *power-additive* if its six edges satisfy

$$d_{ij}^k = u_i + u_j \tag{4}$$

for four real vertex potentials. This is equivalently equality of the three sums of opposite edge powers. For the base set

$$u_A = \frac{b^k + c^k - a^k}{2}, \quad u_B = \frac{c^k + a^k - b^k}{2}, \quad u_C = \frac{a^k + b^k - c^k}{2}. \tag{5}$$

These potentials need not be positive. Let E have columns $B - A, C - A$ in orthonormal planar coordinates, and set $Q = E^\mathsf{T} E$. For $t > t_0 := -\min(u_A, u_B, u_C)$ put

$$d_i(t) = (t + u_i)^{2/k}, \tag{6}$$

$$v(t) = \frac{1}{2}\begin{pmatrix} c^2 + d_A(t) - d_B(t) \\ b^2 + d_A(t) - d_C(t) \end{pmatrix}, \tag{7}$$

$$P(t) = A + EQ^{-1}v(t), \tag{8}$$

$$W(t) = d_A(t) - v(t)^\mathsf{T} Q^{-1} v(t). \tag{9}$$

Here d_i denotes a *squared* apex distance, not an edge length.

Theorem 5.3 (Power-strand theorem)**.** *All nondegenerate power-additive completions of ABC are exactly*

$$D_\pm(t) = P(t) \pm \sqrt{W(t)}\, n, \qquad t > t_0, \quad W(t) > 0. \tag{10}$$

On each admissible interval these are analytic embedded curves. The parameter $t = u_D$ is invariant under base relabelling and scales as length to the power k; $\tau = t/s^k$ is dimensionless. Thus (10) is an equivariantly parametrized strand. For every $k > 1$ and every nondegenerate base, all sufficiently large t are admissible. The power-additive tetrahedral family is a smooth four-dimensional family, and its fixed-base map is a submersion everywhere.

Proof. Equation (4) fixes the three base potentials uniquely and requires $|D - A_i|^2 = d_i(t)$. Subtracting these equations determines $P(t)$ through $E^\mathsf{T}(P - A) = v$; the remaining equation gives $h^2 = W$. This proves necessity, sufficiency, and absence of additional mirror branches. The parameter is recoverable from an apex as $t = |D - A|^k - u_A$, so the curve is injective. Its derivative cannot vanish because $d'_A(t) > 0$; the inverse parameter is continuous. Analyticity holds on $t > t_0$, $W > 0$.

For the tail assertion set $p = 2/k < 2$. As $t \to \infty$,

$$d_i(t) = t^p + pu_i t^{p-1} + O(t^{p-2}), \quad v(t) = O(1 + t^{p-1}).$$

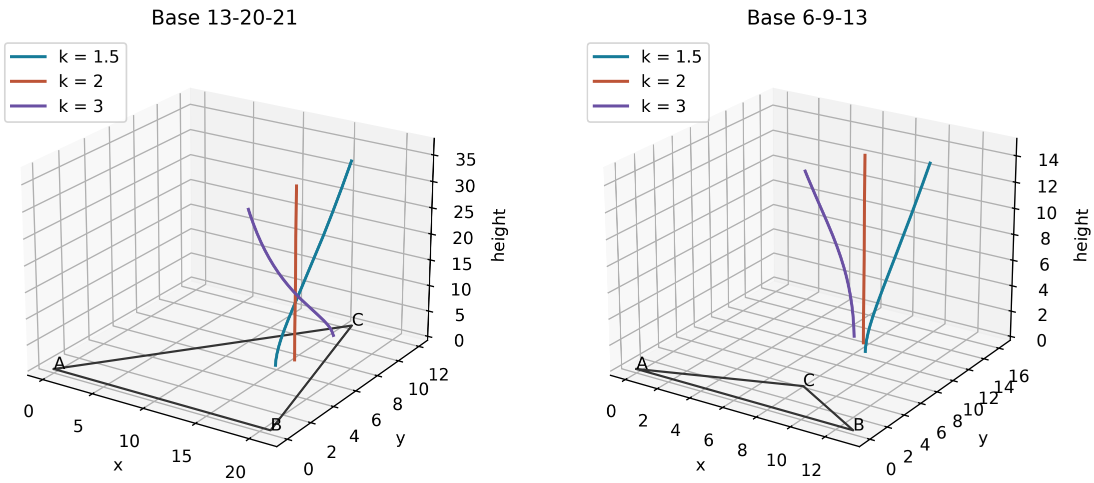

Figure 2: Computed upper-half-space power strands for two fixed bases, using $\tau = t/s^k$. The $k = 2$ strand is vertical; the other displayed exponents give curved loci. Each panel shows only $-\min(u_i)/s^k < \tau \leq 1.5$, and only samples with $W > 0$; the mirror strands are omitted. These are illustrative finite windows, not certified component counts.

Since both $1 = o(t^p)$ and $t^{2p-2} = o(t^p)$,

$$W(t)/t^p \longrightarrow 1. \tag{11}$$

In particular $W > 0$ eventually and the height tends to infinity. Finally (a, b, c, t) are smooth local coordinates on the open admissible set given by (9); they have a smooth inverse from the edge lengths. Forgetting t has rank three, proving the family and submersion assertions. □

No assertion that the admissible set is a single interval is needed. Equation (11) also gives $|P(t) - A|/\sqrt{W(t)} \to 0$: the remote strand becomes asymptotically vertical relative to its height, although its horizontal displacement need not stay bounded.

Corollary 5.4 (Linear and quadratic specializations)**.** *For $k = 2$, the strand is precisely the normal line through H, with*

$$P(t) = H, \qquad W(t) = t - \chi, \qquad t > \chi.$$

For $k = 1$, the foot $P(t)$ is affine in t and $W(t)$ is a quadratic polynomial. Its nonvertical components lie on a conic in a vertical plane; a constant foot gives a vertical-line locus. Only the parts with $t > t_0$ and $W(t) > 0$ are real tetrahedra.

Proof. At $k = 2$, $u_i = \sigma_i$. The distance differences are the altitude equations and $|H - A|^2 = \sigma_A + \chi$, giving the result. The inequality $t > \chi$ implies $t + \sigma_i > 0$. At $k = 1$, $d_i = (t + u_i)^2$; their differences are affine, and substitution in (9) gives the stated degrees. If $P(t) = P_0 + tV$ with $V \neq 0$, the linear coordinate along V and height satisfy a quadratic equation. □

Power-additivity is an edge-family condition. An equal-detour point is a separate point associated with a tetrahedron; it must not be confused with the moving apex in (10). The companion power-k project [2] studies that additional closure problem.

5.2 What a strand visualization should certify

A useful interactive picture displays the base, foot locus, both mirror apex loci, the invariant parameter, and the sign of W. It must keep disconnected admissible intervals separate rather than joining samples across $W \leq 0$. A simple root of W is a square-root height endpoint; multiple roots require separate analysis. For a family given by two implicit edge constraints, the analogue of (9) may be unavailable, but the rank hypothesis of Proposition 5.2 still provides the local test.

For other tetrahedral families, explicit defining constraints and branch conventions are required before the same fiber and Jacobian framework can be applied. Moreover, a point on a general symmetric fiber need not itself be a label-independent center rule until an equivariant parameter is established.

6 Traces, affine closure, and the experimental catalogue

Choose consistently oriented representatives $D = P + hn$ and $E = Q + gn$ of two real stars, with $h, g > 0$. Direct line-plane intersection gives

$$T_- = \frac{gP - hQ}{g - h} \quad (g \neq h), \qquad T_+ = \frac{gP + hQ}{g + h}. \tag{12}$$

The latter is the trace of the line joining D to the mirror of E. If $g = h$ and $P \neq Q$, the ordinary line is parallel to the base; if also $P = Q$, there is no uniquely determined joining line. The cross-conjugate trace is always defined for real positive heights, and lies on the segment PQ.

Proposition 6.1 (Affine trace closure)**.** *Where defined, both traces are triangle centers. If the feet lie in a common affine subspace of the reference plane, the traces remain there. If $h = \alpha q_0$ and $g = \beta q_0$ with a common nonzero height factor and constant coefficients, the trace coefficients are the constants $\beta/(\beta \mp \alpha)$ and $\mp\alpha/(\beta \mp \alpha)$. In particular, rational affine center families are preserved by rational height ratios.*

Proof. Both expressions in (12) are affine combinations whose coefficients sum to one. They commute with similarities and relabellings because the feet and height ratios do. Substitution of the common height factor proves the final assertion. □

This explains a mechanism behind the catalogue's Euler-line concentration: starting with Euler-line feet and applying these trace operations cannot leave that line. High occurrence counts in such a subfamily should not be treated as independent evidence of unexplained center coincidences.

A second useful family has cyclic barycentrics

$$f_A = A_0 + B_0 \frac{a}{s} + C_0 \Phi_A, \quad \Phi_A = a\left(\frac{1}{s-b} + \frac{1}{s-c} - \frac{1}{s-a}\right), \tag{13}$$

where A_0, B_0, C_0 are fixed constants and the symbol A_0 is not a vertex. Let $D_0 = 3A_0 + 2B_0 + 6C_0 \neq 0$.

Proposition 6.2. *The point defined by (13) is*

$$\frac{3(A_0 + 2C_0)}{D_0} G + \frac{2(B_0 - C_0)}{D_0} I + \frac{2C_0}{D_0} L, \qquad L = 2O - H. \tag{14}$$

This defines a rational triangle-center function on every nondegenerate triangle; no database identification is needed to establish its center property.

Proof. Writing $x = s - a$, $y = s - b$, $z = s - c$ proves by expansion that $\sum \Phi_i = 6$. In normalized barycentrics the de Longchamps point satisfies

$$l_A = \Phi_A/2 - 1 + a/(2s),$$

cyclically. One verifies this directly from $L = 2O - H$ using $O = 0$, $H = A + B + C$, or by clearing the nonzero Heron factors xyz. Thus $\Phi_A = 2 + 2l_A - a/s$. Substituting into (13), dividing by D_0, and using the normalized coordinates of G and I proves (14). □

For instance the catalogue candidate U8 is exactly $7G/8 + I/8$, with barycentrics $(7p + 3a : 7p + 3b : 7p + 3c)$, $p = 2s$. An independently executed symbolic check of the twelve supplied expanded center functions against (14) is included with this paper. This validates their algebraic descriptions, not every claimed geometric occurrence or their absence from the ETC.

6.1 The scope of the numerical evidence

The supplied July 2026 audit records 173 stars, including six optimization candidates, against a searchable snapshot of 72,486 ETC entries. It reports 25 distinct matched feet, 371 distinct ordinary-trace matches, 297 distinct cross-conjugate-trace matches, and 524 distinct centers in the union of the two trace families. Their reported intersection has size 144. The report further records 383 recovered trace centers on the Euler line, and 702 repeated unmatched fingerprint classes across three test triangles.

These are dated numerical classifications at tolerance 10^{-9}, not generic projective identities. A successful comparison on several triangles can disprove an identity when it fails, but does not prove an identity when it succeeds. In complex projective matching, all coordinate ratios must be compared with one common scalar; absolute values or selected phases can destroy information. Near-zero denominators and exceptional loci must be treated separately.

The report's score $(\sum_j c_j^{-1})^{-1}$ depends on assigned costs and judgments about independence. It is a discovery-ordering device, not an invariant of a geometric object. We retain the catalogue in the original research archive rather than burden this paper with thirty formula cards and provisional independence counts. Exact claims retained here have proofs or explicitly delimited symbolic checks.

7 Canonical orthocentric completions in four-space

Here the ambient space is genuinely $\mathbb{R}^4$. Embed the base in its first two coordinates and write two added vertices as

$$D = (d, z, 0), \qquad E = (e, u, w), \qquad z, w > 0.$$

These are Gram–Schmidt coordinates in the normal plane, not an extra restriction on a nondegenerate ordered completion. The four-volume is

$$V_4 = \frac{\Delta z w}{12}. \tag{15}$$

Normal-plane isometries do not affect the feet d, e or projections of canonical simplex centers. Proposition 2.2 therefore applies to uniquely selected completions modulo that gauge, and modulo exchange of the added vertices where appropriate.

A simplex is orthocentric precisely when every pair of disjoint edges is perpendicular [8]. One can impose this by minimizing the sum of the fifteen squared normalized disjoint-edge scalar products. The following theorem shows that the minimum is zero for every base, including obtuse and right triangles.

Theorem 7.1 (Volume-normalized orthocentric completion)**.** *Fix a dimensionless constant $\eta > 0$ and impose $V_4 = \eta\Delta^2$. Among orthocentric completions, minimize the normal energy $z^2 + u^2 + w^2$. There is a unique solution in the positive gauge:*

$$d = e = H, \quad c_0 = 12\eta\Delta, \quad z = (\chi^2 + c_0^2)^{1/4}, \quad u = -\chi/z, \quad w = c_0/z. \tag{16}$$

It is nondegenerate for every nondegenerate base and has $u^2 + w^2 = z^2$. Thus it also uniquely solves the lexicographic problem of first minimizing the orthocentric defect and then minimizing the normal energy at the prescribed volume.

Proof. Conditions such as $AB \perp CD$ and $AC \perp BD$ force the foot d to satisfy the base altitude equations, so $d = H$. The same reasoning gives $e = H$. With those feet all disjoint-edge products involving a base edge vanish. The remaining products, up to sign, equal $\chi + zu$. Hence orthocentricity is exactly $zu = -\chi$. Equation (15) gives $zw = c_0$, so every orthocentric completion at this volume is parametrized by $z > 0$, with $u = -\chi/z$, $w = c_0/z$. Its energy is

$$z^2 + \frac{\chi^2 + c_0^2}{z^2} \geq 2\sqrt{\chi^2 + c_0^2},$$

with equality uniquely at (16). This proves existence, global minimality and uniqueness simultaneously. □

For an equilateral base of side ℓ, the calibration $\eta = \sqrt{5}/18$ gives the regular 4-simplex. Indeed $\Delta = \sqrt{3}\ell^2/4$, $\chi = -\ell^2/6$ and (16) gives $z^2 = 2\ell^2/3$ and $|D - E|^2 = 2(z^2 + \chi) = \ell^2$; all remaining edges also have length ℓ.

7.1 Projected centers and a nonsingular incenter formula

For every nondegenerate completion, not just an orthocentric one,

$$\pi(O_4) = O, \qquad \pi(G_4) = \frac{3G + d + e}{5}.$$

The first statement follows by subtracting the circumcenter equations at the three base vertices. In dimension four the Monge point is

$$M_4 = (5G_4 - 2O_4)/3.$$

For an orthocentric simplex it equals its orthocenter. In (16) these identities give

$$\pi(G_4) = \frac{3G + 2H}{5}, \qquad \pi(M_4) = H. \tag{17}$$

To express the incenter without reciprocal singularities at right triangles, use

$$h_A = \frac{\sigma_B \sigma_C}{4\Delta^2}, \quad h_B = \frac{\sigma_C \sigma_A}{4\Delta^2}, \quad h_C = \frac{\sigma_A \sigma_B}{4\Delta^2}. \tag{18}$$

The identity $\sigma_A\sigma_B + \sigma_B\sigma_C + \sigma_C\sigma_A = 4\Delta^2$ makes these the normalized barycentrics of H on *every* nondegenerate triangle.

Theorem 7.2 (Projected incenter)**.** *Set $K = z^2 + \chi > 0$ for (16). The tetrahedral facet volumes of the 4-simplex, indexed by the omitted vertex, are*

$$\begin{aligned} F_A &= \frac{1}{6}\sqrt{K(a^2K + 2\sigma_B\sigma_C)}, \quad \textit{cyclically}, \\ F_D &= F_E = \Delta z/3. \end{aligned} \tag{19}$$

Its incenter projects to the triangle center

$$J_\eta = (\Lambda_A : \Lambda_B : \Lambda_C), \qquad \Lambda_A = F_A + \frac{2\Delta z}{3} h_A, \tag{20}$$

cyclically. Equations (18)–(20) extend directly across right triangles without division by a vanishing σ_i.

Proof. The two facets on base ABC have equal normal height because $u^2 + w^2 = z^2$. In the facet $BCDE$, the Gram matrix of $B - D, C - D, E - D$ is

$$\begin{pmatrix} K + \sigma_B & K & K \\ K & K + \sigma_C & K \\ K & K & 2K \end{pmatrix}.$$

Its determinant is $K(a^2 K + 2\sigma_B \sigma_C)$, since $\sigma_B + \sigma_C = a^2$. Taking the square root and dividing by 6 proves (19). All radicands are positive because the constructed simplex is nondegenerate. The incenter is the facet-volume-weighted mean of the five vertices. Projection, $d = e = H$ and (18) give (20). Its coordinate sum is $F_A + F_B + F_C + 2\Delta z/3 > 0$, including at right triangles. $\square$

These are normalized signed barycentrics after division by their sum. Individual components need not be presumed positive merely because the original 4-simplex incenter is interior: the projected convex hull also contains the two apex feet.

The centroid in (17) has homogeneous coordinates

$$\Gamma_A = 3\sigma_B \sigma_C + \sigma_C \sigma_A + \sigma_A \sigma_B, \quad \text{cyclically.}$$

Expansion gives $4\Gamma_A = a^4 + 2a^2(b^2 + c^2) - 3(b^2 - c^2)^2$, identifying it exactly as $X(3091)$ from the published ETC formula [5]. This identification is symbolic, unlike the larger numerical census.

7.2 Center-proximity selection and its boundary

An alternative selection dispenses with a prescribed volume and minimizes the distance between the simplex orthocenter and centroid within the orthocentric completion family. Denote these centers by K_4, G_4. With horizontal origin H and $o = O - H$, direct circumcenter subtraction gives

$$G_4 = (2o/5, (z + u)/5, w/5), \qquad K_4 = (0, u, u(z - u)/w), \quad zu = -\chi.$$

Thus

$$25|K_4 - G_4|^2 = 4|OH|^2 + (4u - z)^2 + \frac{(5u(z - u) - w^2)^2}{w^2}. \tag{21}$$

Distances between any other two of K_4, G_4, O_4 differ by constant factors, so they select the same minimum.

Theorem 7.3 (Center-proximity completion)**.** *For every nonright base there is a unique nondegenerate minimum of* (21) *in the positive gauge. Its normal coordinates are*

$$(z, u, w) = \begin{cases} (2\sqrt{-\chi}, \sqrt{-\chi}/2, \sqrt{15(-\chi)}/2), & \chi < 0, \\ (\sqrt{6\chi}, -\sqrt{\chi/6}, \sqrt{35\chi/6}), & \chi > 0. \end{cases} \tag{22}$$

At a right triangle the infimum is not attained nondegenerately. The projected incenter nevertheless extends continuously from both sides to the right-angle vertex.

Proof. For $\chi < 0$, $u > 0$, and both variable squares in (21) vanish exactly when $z = 4u$, $w^2 = 15u^2$. Combining with $zu = -\chi$ gives the first formula. For $\chi > 0$, write $z = \sqrt{\chi}\, t$ and $u = -\sqrt{\chi}/t$. For fixed t, minimizing the last term over $w > 0$ gives $w^2 = -5u(z - u)$. The remaining variable contribution is

$$\chi(t^2 + 28 + 36/t^2),$$

uniquely minimized at $t^2 = 6$. If $\chi = 0$, then $u = 0$ and the variable contribution is $z^2 + w^2$, with unattained infimum zero.

Both branches satisfy $u^2 + w^2 = z^2$, so Theorem 7.2 applies with $K = -3\chi$ on the acute branch and $K = 7\chi$ on the obtuse branch. Suppose the limiting right angle is at A. Then $\sigma_A \to 0$,

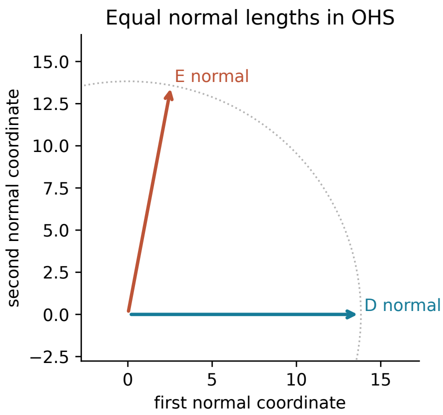

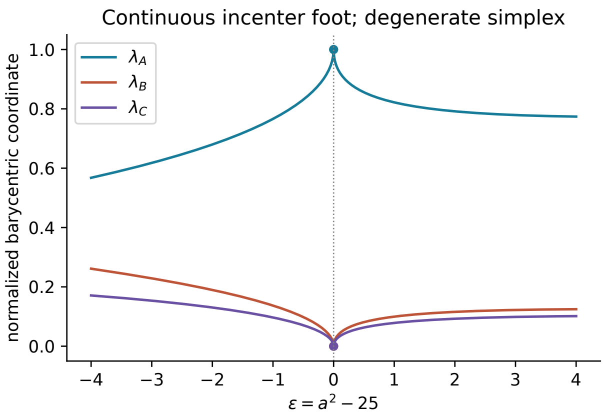

Figure 3: Normal-plane coordinates of the energy-balanced completion over the 13–20–21 base at $\eta = \sqrt{5}/18$ (left); both feet equal H, and the two normal vectors have equal length. Projected incenter barycentrics of the center-proximity completion along $(a, b, c) = (\sqrt{25+\epsilon}, 4, 3)$ (right) tend to $(1, 0, 0)$ as $\epsilon \to 0$ from either side. The plot shows planar descendants, not a nondegenerate simplex at $\epsilon = 0$.

σ_B, σ_C tend to positive numbers, and $(h_A, h_B, h_C) \to (1, 0, 0)$. Since $\chi = -\sigma_A\sigma_B\sigma_C/(4\Delta^2)$, one has $\sigma_A = O(|\chi|)$ locally. Consequently F_A and Δz are positive constants times $\sqrt{|\chi|}$ to leading order, whereas $F_B, F_C = O(|\chi|)$ and $zh_B, zh_C = o(\sqrt{|\chi|})$. Dividing (20) by its sum therefore gives $(1, 0, 0)$ from either side. □

The selected volume satisfies

$$12\eta\Delta = zw = \begin{cases} \sqrt{15}(-\chi), & \chi < 0, \\ \sqrt{35}\chi, & \chi > 0. \end{cases}$$

Thus center proximity selects a triangle-dependent member of the energy-balanced family, not one universal fixed-volume member. At a right triangle the simplex degenerates even though its projected incenter has the continuous value just proved. This distinction matters when plotting a center across the acute–obtuse boundary.

8 Reproducibility and remaining questions

The accompanying archive provides this manuscript, vector figure sources, independent symbolic and numerical checks, a critique and change map, and the unmodified supplied report archive. Symbolic verification includes the twelve affine center functions, the primitive-height identity, facet determinants, the $X(3091)$ identity, and optimization derivative signs. Numerical checks use multiple acute, obtuse and near-right bases to compare formulas with direct Gram and distance calculations. Numerical samples are consistency checks, not proofs of the global theorems.

All 57 supplied files listed in the original checksum manifest match their recorded hashes; the separately listed report PDF was absent. The complete input needed by the original ranked-catalogue builder, including `TriangleSkyRankedStars.json`, is not supplied. One historical export also uses nonstandard JSON numeric tokens. These issues are recorded in the companion audit; they do not affect the self-contained theorems above. The current paper neither replays nor certifies the complete ETC matching pipeline.

The next mathematical questions are focused. Does the Euler-ratio minimizer have a unique reflection class for every scalene base? Do the fixed-base dihedral and frame objectives attain unique interior minima, and how do their boundary values compare? For power strands, how many components can $W > 0$ have as k and the base vary, and when can multiple zeros occur? For other four-dimensional tetrahedral families, can one prove the rank condition globally and select an invariant strand parameter? Finally, which catalogue coincidences admit proofs independent of the affine closure mechanism? Those problems remain separate from the results proved here.

Assistance and status. This pilot was developed from the author's report with ChatGPT assistance in mathematical derivation, proof drafting, computation and editing. It is not peer reviewed. The author must independently review the new arguments and approve the final manuscript and factual submission declarations before journal submission.

A The twelve affine candidates in the supplied audit

The labels below are internal to the source report, not ETC identifiers. The table collects their constant affine descriptions. The independent symbolic checks establish equivalence with the supplied expanded functions, while the source's occurrence counts and trace provenance remain audit records.

Label	coefficient of G	coefficient of I	coefficient of L
U1	3/8	1/4	3/8
U2	11/16	1/4	1/16
U3	7/8	1/4	−1/8
U4	11/16	1/8	3/16
U5	25/32	1/8	3/32
U6	13/16	1/4	−1/16
U7	3/4	1/8	1/8
U8	7/8	1/8	0
U9	1/2	1/4	1/4
U10	19/32	1/8	9/32
U11	21/32	1/8	7/32
U12	7/16	1/4	5/16

All coefficients in each row sum to one. Their simplicity is mathematically useful, but being an explicit affine combination does not imply that a center is absent from a database or independently novel.

References

[1] I. Hammoudeh, *The Triangle Sky: Triangle centers lifted to a ranked geometry of tetrahedral apices*, living research report, v0.2, 30 August 2026. Supplied source archive; not peer reviewed.

[2] I. Hammoudeh, *Power-k Equal-Detour Points of Triangles and Simplices*, revised working manuscript, September 2026. Related project manuscript; not peer reviewed.

[3] C. Kimberling, Triangle centers and central triangles, *Congressus Numerantium* **129** (1998), 1–295.

[4] C. Kimberling, *Encyclopedia of Triangle Centers*, `https://faculty.evansville.edu/ck6/encyclopedia/`. Database identifications in the supplied audit refer to its July 2026 local snapshot.

[5] C. Kimberling, ETC entry $X(3091)$, Encyclopedia of Triangle Centers, Part 3. Formula checked 6 September 2026.

[6] N. Amenta, M. Bern and D. Eppstein, *Optimal Point Placement for Mesh Smoothing*, 1998, https://arxiv.org/abs/cs/9809081.

[7] P. Colognese and M. Pollicott, *Kneading sequences of triangles and tetrahedra*, manuscript, 11 March 2021, https://warwick.ac.uk/fac/sci/maths/people/staff/mark_pollicott/p3/kneading.pdf.

[8] A. L. Edmonds, M. Hajja and H. Martini, Orthocentric simplices and their centers, *Results in Mathematics* **47** (2005), 266–295; https://arxiv.org/abs/math/0508080.

[9] J. J. Benedetto and M. Fickus, Finite normalized tight frames, *Advances in Computational Mathematics* **18** (2003), 357–385, https://doi.org/10.1023/A:1021323312367.

[10] D. G. Mixon, T. Needham, C. Shonkwiler and S. Villar, Three proofs of the Benedetto–Fickus theorem, in *Sampling, Approximation, and Signal Analysis*, Birkhäuser, 2023, 371–391; https://arxiv.org/abs/2112.02916.